energies

MDPI

Article

Research on Characteristics of ECVT for Power Quality Detection and Optimum Design of Its Parameter

Xingjie Liu, Yamin Zeng *, Baoping An and Xiaolei Zhang

Department of Electrical Engineering, North China Electric Power University, Baoding 071003, China; lxj5085@163.com (X.L.); 2172213182@ncepu.edu.cn (B.A.); 2172213049@ncepu.edu.cn (X.Z.)

* Correspondence: 2172213012@ncepu.edu.cn; Tel.: +86-182-7088-6382

Received: 27 April 2019; Accepted: 17 June 2019; Published: 24 June 2019

check for updates

Abstract: Electronic Capacitive Voltage Transformer (ECVT), connecting the transmission system and measuring device, is the key equipment of digital substation in the distribution network. Its frequency characteristics and the rapid transient response performance exert decisive effects on whether it is in keeping with the power quality requirements for wide frequency domain and high precision detection. Many detection methods that require special testing equipment have limitations of high-cost and complexity in project implementation. We establish the mathematical model of ECVT, which is utilized to study its integrative characteristics based on the definitions of frequency response and transient voltage error. Besides, the harmonic and transient disturbance detection performances are analyzed comprehensively with the model by simulation. Then, we propose a multi-objective parameter optimization design model with minimization of transient voltage decay duration, maximization of frequency bandwidth and minimization of transient impulse voltage, which is solved through the entropy weighting method and genetic algorithm. The analysis and optimization results indicate that selecting resistor divider through the proposed method can achieve data transmission results with acceptable accuracy. Further, its superior performance on transforming transient disturbances conforms to the distribution network's electric energy quality requirements.

Keywords: electronic voltage transformer; harmonics; transient disturbance; parameter optimization

1. Introduction

With the advancement of voltage level and transmission capacity in power system, the problem of electric energy quality is increasingly prominent and complicated for the application of various power electronics devices and the access of energy storage equipment [1]. Thus, this problem is becoming the primary concern for energy companies as serious issues affecting all voltage levels at electrical power networks. It results not only from the necessity to fulfill the requirements of promulgated regulations; it is also a consequence of not satisfying the required standards in the aspects of economy and technology [2].

Harmonic and transient disturbances are two major problems of power quality in distribution networks. As the basic equipment of primary voltage measurement, the accuracy and validity of voltage distortion data and transient disturbance signal provided by the voltage transformer are the decisive basis to determine its measurement accuracy. The traditional electromagnetic voltage transformer makes it easy to produce ferromagnetic resonance with both capacitance and inductive impedance in the line for its iron core [3]. The capacitive voltage transformer distorts the harmonic components in the power network invariably because of its structure [4]. Moreover, it is also tough to accurately reflect the transient disturbance. The Electronic Voltage Transformer (EVT) applies fiber optics to transmit signals, thereby achieving complete electrical isolation of high and low voltage. EVT has the features of high linearity, simple structure and resistance to electromagnetic interference, which ensure the accuracy and validity during data processing [5]. Among them, Electronic Capacitive Voltage Transformer (ECVT) is utilized widely for its precise capacitive voltage divider and mature actual production technology [6].

At present, the research about ECVT mainly focuses on satisfying the requirements of fundamental wave measurement and relay protection. Insufficient consideration is given to the power quality detection needs [7–10]. Paper [11] presents the analysis results of the impact of secondary voltage divider on ECVT's transient characteristics and its corresponding grade. On this basis, the effect of capacitor internal resistance is considered in reference [12]. When the ratios between high-low capacitor series resistance and voltage are equal, ECVT can obtain a relatively exact transmission result. The paper [13] established the transfer function model of ECVT to attain its measurement performance for various disturbance signals problems effectively. The results showed that ECVT has excellent restoration capacity for the primary signal. The authors of the article [14] discussed a similar issue by illustrating the analysis of the harmonics measurement accuracy within the normal measuring frequency domain, which was conducted in designed test circuits. Related research [15] shows that the capacitive tap in current transformer bushings, applied to power networks, can solve harmonic voltage measurement problems with comparatively precise results. However, the capacitive tap has the drawback of always being affected by the potential transformer. Moreover, it is not efficient when a resistor or nonlinear resistor is connected across the neutral point of the primary side and ground. The resistive voltage divider is applied in [16] to settle the voltage harmonics measurement problem of the transmission network of 400 kV. It has better performance than inductive voltage transformer and capacitive voltage transformer in terms of measurement error. It is effective to apply its internal parameters to optimize the frequency and transient characteristics of ECVT to attain the minimum voltage error [17].

The above research either discusses the transient characteristics of ECVT voltage divider from the perspective of its internal structure and the corresponding parameter value level, ignoring its impact on frequency bandwidth or analyzes its metering transmission performance from the perspective of ECVT signal measurement application. Therefore, how to comprehensively receive the influence regulation of sensor parameters on ECVT and its value range, from the perspective of the overall structure combined with the traits of transient process and harmonic signal measurement, is of great significance for promoting its real application in power network. Based on the overall structure and working principle of ECVT, by constructing the corresponding equivalent circuit model, this paper presents the theoretical analysis of its transient conditions and transfer characteristics which is verified by simulation. Further analysis is mainly focused on the impacts of the resistor divider on solving the issue of retained charge and primary short circuit. The influence of its range on the harmonic measurement performance is discussed. To improve the power quality detection ability of ECVT, the value of resistor divider is selected reasonably. The models of coaxial capacitive voltage divider and integrating circuit in ECVT are established in Section 2; The transient and transfer characteristics analysis of ECVT is introduced in Section 3; The simulation analysis of short circuit, reclosing and harmonic transmission are presented in Section 4; The parameter optimization design model is described in Section 5; The discussion about the simulation and optimization results is given in Section 6; Finally, conclusions are drawn in Section 7.

2. Models of ECVT

The general frame of ECVT includes three parts: the primary voltage sensor, the secondary signal acquisition circuit, and the processing system of the secondary signal [18]. The specific structure of ECVT is presented in Figure 1.

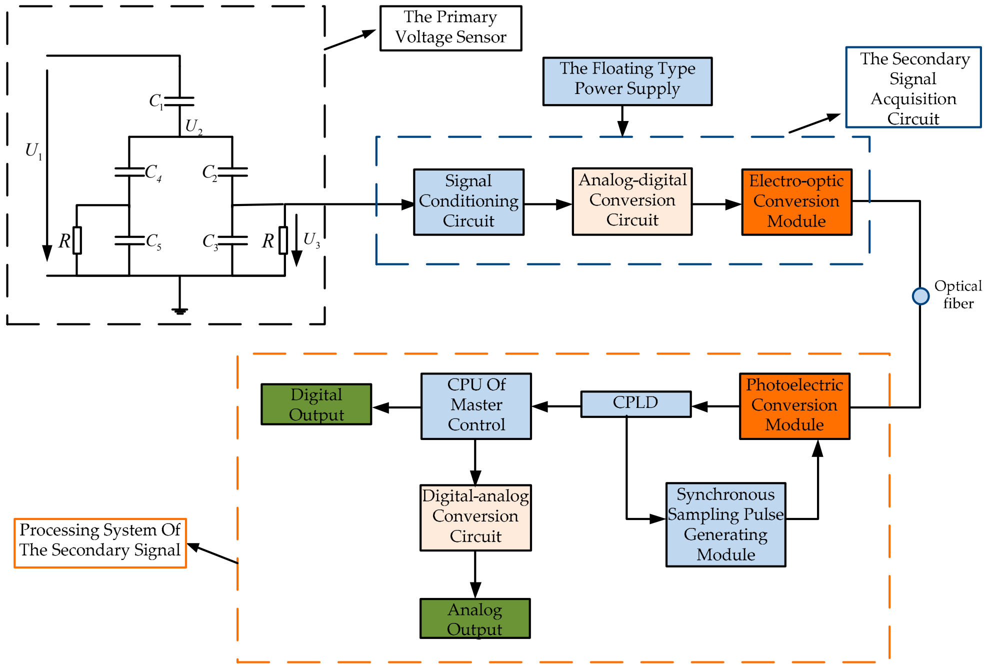

Figure 1. Structural schematic diagram of Electronic Capacitive Voltage Transformer (ECVT).

The coaxial capacitive voltage divider is applied to convert high voltage into low voltage. Then the measured voltage signal is modulated and analog-to-digital converted by the secondary signal acquisition circuit. Then the electrical signal is converted into the optical signal, which is transmitted to the secondary signal processing system through optical fiber and recovered by photoelectric conversion. Finally, the message is processed and output in the form of analog or digital signals [19–21].

The capacitive voltage divider is the core of ECVT to realize the function of power measurement, which is composed of three coaxial metal cylinders with the radius of r_1, r_2 and r_3 respectively. The inner one is connected to a high voltage conducting rod. The intermediate one is attached to the divider resistance of secondary side voltage, and the outer one is grounded [22–24]. The structural schematic diagram and equivalent circuit model are illustrated in Figure 2.

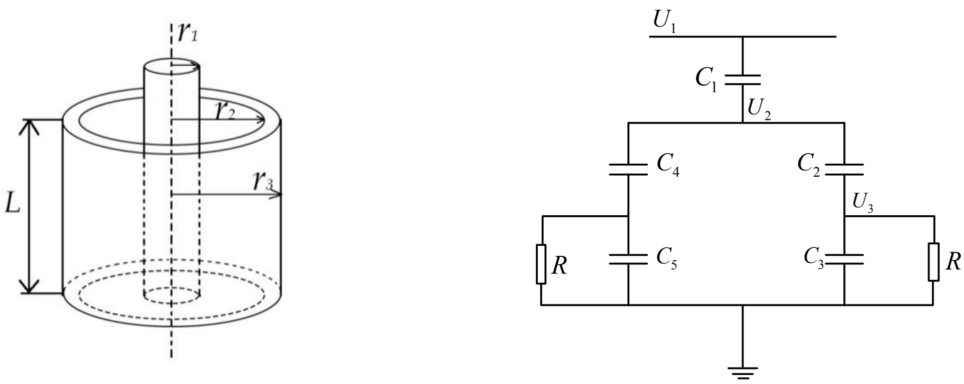

(**a**) (**b**)

Figure 2. (**a**) The structure of coaxial capacitive and (**b**) the equivalent circuit model of voltage divider.

Among them, U_1 is high side voltage; U_2 is intermediate electrode voltage; U_3 is secondary side voltage; R is the resistor divider of secondary side voltage; C_1 is the high voltage side capacitance; C_2 is intermediate electrode capacitors; C_3 is low voltage side capacitors; C_4 equals to C_2; C_5 equals to C_3.

Secondary side voltage U_3 can be denoted by

$$U_3 = \frac{jwRC_1C_2}{C_1 + 2C_2 + jwR(C_1C_2 + C_1C_3 + 2C_2C_3)} \tag{1}$$

The voltage ratio K and phase deviation $\Delta\theta$ can be described as

$$K = \left|\frac{U_1}{U_3}\right| = \left|\frac{C_1 + 2C_2}{jwRC_1C_2} + \frac{C_1C_2 + C_1C_3 + 2C_2C_3}{C_1C_2}\right| \tag{2}$$

$$\Delta\theta = 90^\circ - \theta_1 \tag{3}$$

$$\theta_1 = \arctan\left[\frac{wR(C_1C_2 + C_1C_3 + 2C_2C_3)}{C_1 + 2C_2}\right] \tag{4}$$

In practical calculation, the value of θ_1 is very small. The phase offset of secondary side voltage U_3 leading voltage U_1 is close to 90 degrees [25]. Therefore, Equation (1) can be approximated as

$$U_3 \approx \frac{jwRC_1C_2}{C_1 + 2C_2} U_1 \tag{5}$$

According to Equation (5), the voltage U_3 is proportional to the differential of the input voltage U_1. The proportional integral processing is required to get the voltage signal linearly correlated with the input voltage. Further, the value of K is determined by the values of R, C_1 and C_2. Furthermore, when K is assumed to be constant, parameter R is adjusted to realize the signal transmission for different voltage levels.

ECVT generally adopts the active feedback RC external circuit containing high performance operational amplifier to realize integral function in its practical application [26]. Its equivalent circuit diagram is exhibited in Figure 3.

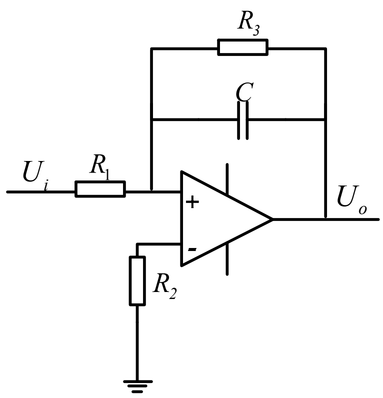

Figure 3. Structural schematic diagram of active feedback analog integrator.

Among them, U_o is the output voltage; C is the integral capacitance; R_3 is the integral feedback resistance (the integral drift voltage is slowly accumulated and released through it to keep the circuit working point stable). The relation between the input and output voltage of the integrator can be described as

$$\frac{U_o}{U_3} = -\frac{R_3}{R_1(1 + sCR_3)} \tag{6}$$

To ensure the safe and stable operation of the integrator, the feedback resistance in parallel with the integrator capacitor is usually the one of megohm level. Then, it can be inferred that $sCR_3 \gg 1$ and Equation (3) can be simplified to

$$U_o \approx -\frac{U_3}{sCR_3} \tag{7}$$

At this point, the input and output voltage signals form an approximate integral relationship, to achieve signal restoration. The equivalent circuit of the primary voltage sensor, composed of the capacitive voltage divider and the active negative feedback analog integrator, is shown in Figure 4.

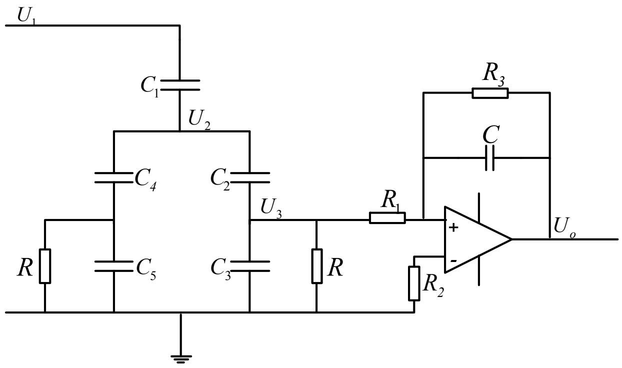

Figure 4. The equivalent circuit of primary voltage sensor.

Based on the integral circuit principle, the overall system transfer function is as follows

$$H(s) = \frac{U_o}{U_3} \cdot \frac{U_3}{U_1} = -\frac{R_3}{R_1(1 + sCR_3)} \cdot \frac{sC_1C_2R}{C_1 + 2C_2 + sRC_n} \tag{8}$$

The amplitude-frequency and phase-frequency characteristics of ECVT can be expressed as

$$\left|H(jw)\right| = \frac{R_3}{\sqrt{R_1{}^2 + w^2C^2R_3{}^2)}} \cdot \frac{wC_1C_2R}{\sqrt{(C_1 + 2C_2)^2 + w^2R^2C_n^2}} \tag{9}$$

$$\Delta\theta = 180^\circ - \arctan(wCR_3) + 90^\circ - \arctan\left(\frac{wRC_n}{C_1 + 2C_2}\right) \tag{10}$$

where $C_n = C_1C_2 + C_1C_3 + 2C_2C_3$.

Because the high and low voltage sides are electrically isolated by optical fibers, the signal transmission property remains static under the signal processing link of subsequent digital-to-analog conversion [21]. Thus, this paper focuses on characteristic analysis of its analog signal processing circuit.

3. Characteristics Analysis of ECVT

3.1. Transient Characteristics Analysis of ECVT

Because there is no ferromagnetic resonance problem in ECVT, its transient response characteristics are illustrated emphatically in this paper. Consulting the division of IEEE std.1159-2009 power quality standard, the primary side to ground short circuit and the reclosing with trapped charge are the typical power quality transient conditions. With the reference to standard GB/T 20840.7-2007, voltage error ε is taken as a measure of the transient characteristics, which is required to be less than 10% within 2–3 cycles of the rated frequency after the transient process.

$$\varepsilon = \frac{\sqrt{2}U_3' - U_{3\max}}{\sqrt{2}U_3'} \times 100\% \tag{11}$$

where $U_{3\max}$ is the maximum value of the secondary side voltage and U'_3 is the rated effective value of it under steady state.

3.1.1. The Transient Process of Short Circuit

When the transformer is short circuited on the primary side, the charge on the capacitor, discharge through the partial voltage resistance and transmit to the secondary side, causes the output voltage to contain transient components and results in voltage errors [27].

When the circuit is in the normal state, suppose the expression of its primary side voltage is

$$U_1(t) = \sqrt{2}U_m \cdot \sin(2\pi f_n t + \varphi_0) \tag{12}$$

The output voltage of the transformer is

$$U_o(t) = -\frac{1}{CR_1} \cdot \frac{RC_1C_2}{C_1 + 2C_2} \cdot \sqrt{2}U_m \sin(2\pi f_n t) \tag{13}$$

Assume that the voltage reaches its peak at time t, and a grounding short circuit occurs at the high voltage side. Then, the transient voltage at the secondary side is

$$U_3(t) = \sqrt{2}U_m \cdot \frac{RC_1C_2}{C_1 + 2C_2} \cdot 2\pi f_n \cdot \sin(2\pi f_n t + 90^\circ) \cdot e^{-t(C_1+2C_2)/RC_n} \tag{14}$$

After the inverse Laplace transform of the transient output voltage obtained through the integrator, the following formula can be obtained:

$$U_o(t) = -\sqrt{2}U_m \cdot \frac{RC_1C_2}{C_1 + 2C_2} \cdot \sin(2\pi f_n t) \cdot \frac{1}{CR_1} \cdot \frac{RC_n}{C_1 + C_2} \cdot \left(1 - e^{-t(C_1+2C_2)/RC_n}\right) \tag{15}$$

The disturbance degree depends on the impulse voltage and discharge time. When the capacitance of the high and low voltage side has been determined, the change of its integral capacitance will exert effect on its voltage amplitude. While the resistor divider R focuses on the impact of its time constant.

3.1.2. The Transient Process of Reclosing

When the line or cable is suddenly disconnected during operation of the ECVT, the charge stuck on C_1 is hard to release. It will cause the charge transfer phenomenon of the voltage divider after reclosing, which clearly produces error interference to the later circuit [28].

The amount of trapped charge is subject to the voltage phase at the time of disconnection. Assume that the voltage reaches its peak at time t_0, and at the same time, the ECVT is disconnected from power grid. When the voltage reaches its trough peak at time t_1, the ECVT is reclosed to power grid. Then the capacitors C_1, C_2 and C_4 will store charge and the low voltage capacitors C_3 and C_5 will release charge through the shunt partial voltage resistors. After reclosing, the low DC impedance lines of the grid discharge immediately, forcing the charge to transfer to C_3 until its voltage reaches $C_1C_2U_\mathrm{m}/C_\mathrm{n}$. The voltage will be exponentially attenuated with the time constant equals RC_3 and superimposed on the steady state sine wave signal, which could result in voltage deviation.

Within the time interval of reclosing operation, the charge in C_3 is discharged through the external partial voltage resistance R. Furthermore, the representation of U_3 after Laplace transformation is:

$$U_3(s) = \frac{RC_1C_2}{C_1 + 2C_2} \cdot \sqrt{2}U_m \cdot 2\pi f_n \cdot \sin(2\pi f_n t_0 + 90^\circ) \cdot e^{t_0/RC_3} \cdot \frac{RC_3}{1 + sRC_3} \tag{16}$$

where t_0 represents the time when the line is disconnected.

Transient voltage error formed by the voltage side after reclosing:

$$\Delta u_3(t) = -\frac{C_1C_2}{C_n} \cdot U_m \cdot 2\pi f_n \cdot \sin(2\pi f_n t_0 + 90^\circ) \cdot e^{-(t-t_1)/RC_3} \tag{17}$$

After reclosing, the output voltage signal is:

$$U_o(t) = -\frac{U_m}{CR_1} \cdot \left(\frac{RC_1C_2}{C_1 + 2C_2} \cdot \sqrt{2}\sin(2\pi f_n t) - \frac{C_1C_2}{C_n} \cdot RC_3 \sin(2\pi f_n t_0) \cdot e^{t_1/RC_3} \cdot (1 - e^{t/RC_3}) \right) \quad (18)$$

where t_1 stands for the time when the line is closed.

Combined with Equations (14) and (15), it is found that voltage error and the discharge time of trapped charge are affected by the value of the resistor divider R. Furthermore, the superimposed direct flow is caused by voltage difference, created between the high and low voltage capacitor and produced by trapped charge, in the low voltage capacitor. Its value increases with the decrease of R. However, after reclosing, the discharge time diminishes with the decrease of R, which means the voltage error in the transient state decreases similarly.

3.2. Transfer Characteristics Analysis of ECVT

Frequency characteristics of ECVT, obtained from its transmission function, are illustrated in Figure 5. ECVT has the traits of wide frequency band and high linearity (Figure 5). Furthermore, it should be able to precisely measure the harmonic signal with the frequency in its normal measurement frequency range [29–33]. It is known that the amplitude ratio and phase difference of the input and output voltage signals of ECVT at different frequencies and their trend with frequency.

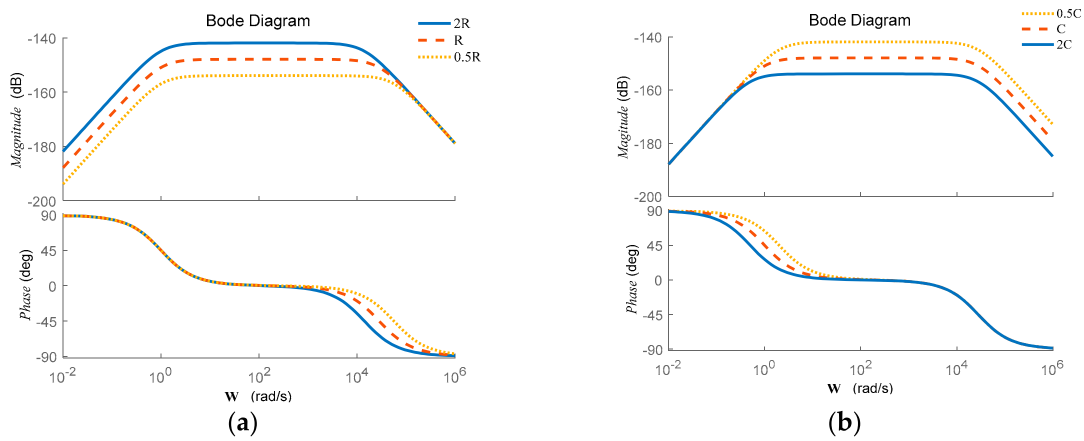

Figure 5. (**a**) Frequency characteristics of different resistances and (**b**) Frequency characteristics of different integral capacitances.

According to Equation (8), the upper frequency f_H and lower frequency f_L of ECVT can be described as

$$f_H = \frac{C_1 + 2C_2}{2\pi RC_n} \quad (19)$$

$$f_L = \frac{1}{2\pi R_3 C} \quad (20)$$

Combined with Figure 5 and Equation (19), the influence of parameters R and C on frequency characteristics of ECVT can be obtained respectively. The initial decay cut-off frequency value and transmission characteristics are shifted with the use of different resistor dividers and integral capacitors. With the increase of parameter R, the upper limit frequency decreases and the transmission characteristic becomes worse. When growing the integral capacitance C, its lower limit frequency decreases and the bandwidth increases. However, the ECVT's transmission capacity depends on the upper limit of the normal measured frequency bandwidth. According to Equation (9), it is related to the value of parameter R in the primary voltage sensor.

4. Simulation Analysis and Optimum Design of ECVT

4.1. Simulation Analysis of Transient Characteristics

Because there is no ferromagnetic resonance problem in ECVT, this paper focuses on analyzing its transient response characteristics as illustrated emphatically [34,35]. The primary side to ground short circuit and the reclosing with trapped charge are analyzed respectively. The simulation model is presented in Figure 6. The reclosing process is determined by switch K_1, and the short circuit process of high voltage terminal is realized by switch K_2. This part is simulated for 10 kV ECVT. Besides, the capacitance values of the capacitance divider are C_1 = 30.5 pF, C_2 = C_4 = 4.98 nF, C_3 = C_5 = 123.2 nF; the rated input voltage is $10/\sqrt{3}$ kV; the integral capacitance is 1 uF.

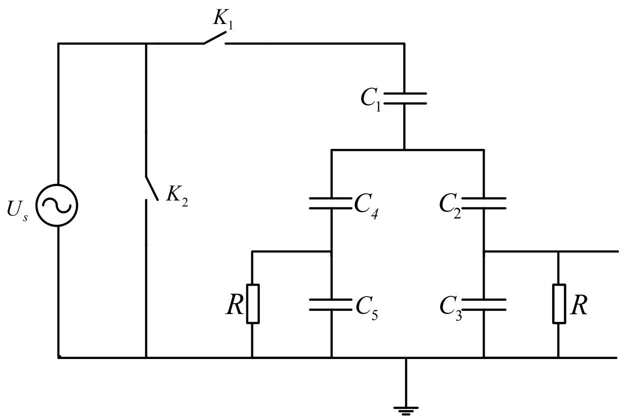

Figure 6. The simulation circuit of ECVT.

4.1.1. Short Circuit

Because the time of the primary side short circuit determines the magnitude of the transient voltage on the second side, the content below is conducted for two representative cases: when short circuit occurs at the peak voltage and across zero [36]. By referring to the EVT standard, the voltage error is required to less than 10% after a period of three cycles under the rated frequency. The transient characteristic of ECVT obtained is demonstrated in Figure 7.

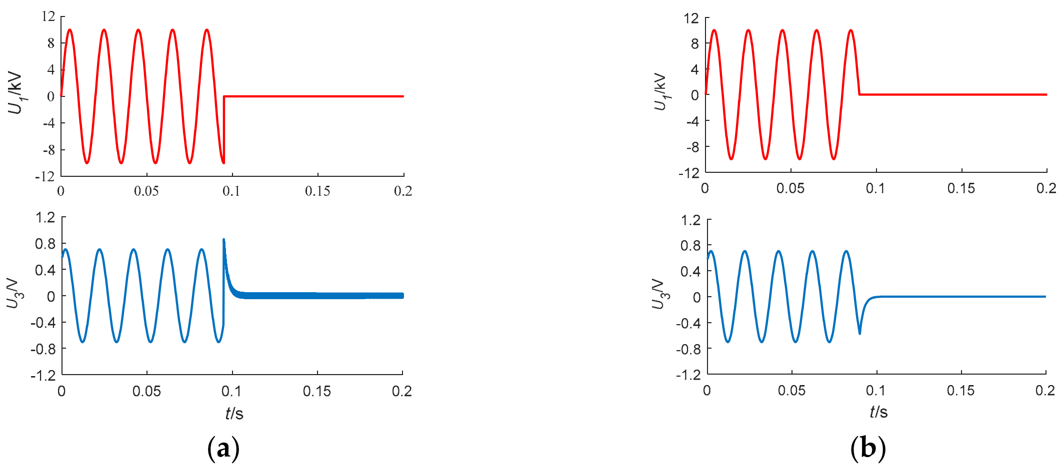

Figure 7. (**a**) Transient characteristics of short circuit at peak time and (**b**) Transient characteristics of short circuit at zero-crossing time.

As can be seen from Figure 7, that charge on the capacitor is released in a short time, which depends on the short circuit time of occurrence and its time constant which is equal to $RC_n/(C_1 + 2C_2)$. Although its transient process is shortened with the decrease of the resistor divider, when its value is too small, it may cause impulse voltage that is released in a brief time. In this process, the impulse voltage may cause irreparable damage to the circuit devices. Therefore, to reduce the charge disparity before and after the transient state, the resistor divider should not be too small. Extract three representative ranges of resistances for simulation and the result is presented in Figure 8.

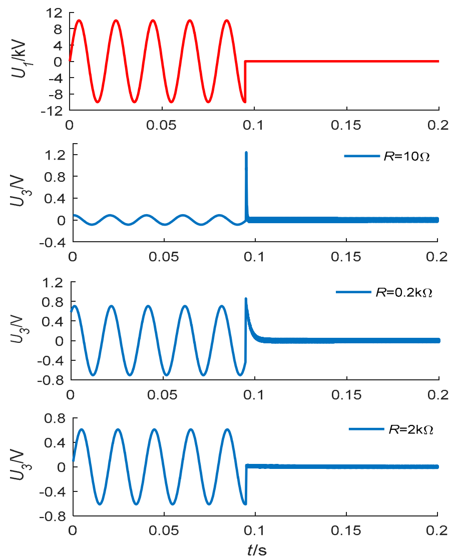

Figure 8. Input and output waveforms for different resistances.

Impulse voltage, produced by short circuit, is 5.31 times as large as steady-state secondary voltage peak (R = 10 Ω). The secondary side voltage is abrupt at the moment of short circuit (R = 0.2 kΩ). The maximum value of the transient impulse voltage is already less than 10% of the steady-state voltage peak (R = 2 kΩ). In summary, the simulation results are consistent with the theoretical analysis. The resistor divider R, in the researched ECVT, should be adjusted to more than 2 kΩ to fulfill the standard requirement of the transformer.

4.1.2. Reclosing

According to the operation experience, regardless of the situation of line disconnection lasting a long time, the upper limit of reclosing action time is about 0.5 s [37,38]. Furthermore, K_1 is disconnected at 0.005 s with 0.15 s as the time interval for reclosing, which is broken at the crest and closed at the trough. When R is 2 kΩ, the waveform of the secondary voltage is exhibited in Figure 9.

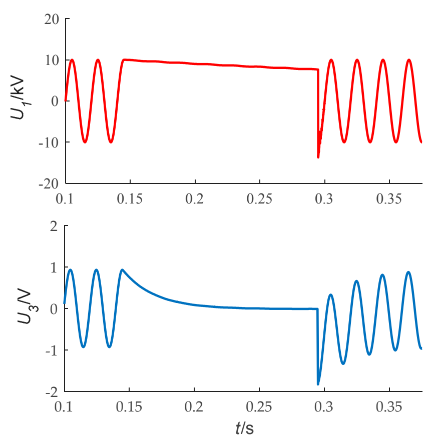

Figure 9. Waveforms of reclosing simulation.

The theoretical study describes that voltage error will change with different partial pressure resistance *R*. So, under the situation that reclosing time interval is 0.15 s, we modify the value of *R* and record voltage error at the voltage peak after closing according to the standards. Finally, we obtain the relationship between resistance *R* and the voltage error by repeated simulation. The result is shown in Figure 10 and Table 1.

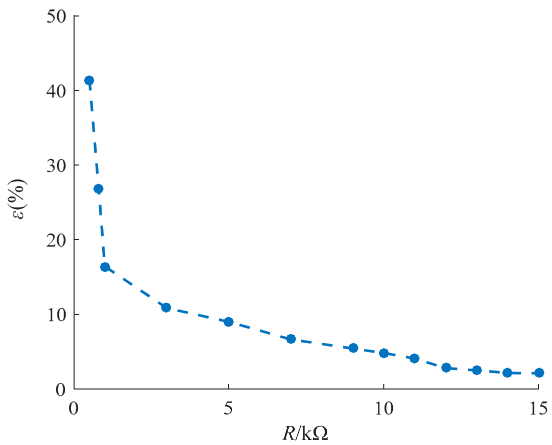

Figure 10. Relationship between resistor divider and the voltage error.

Table 1. Relationship between the resistor divider and voltage error.

R/(kΩ)	ε/(%)	*R*/(kΩ)	ε/(%)
0.1	67.94	7	6.66
0.5	41.40	9	5.83
0.8	26.85	10	5.22
1	13.43	11	3.20
3	10.36	12	2.41
5	9.01	13	2.34

According to the chart above, when the resistor divider *R* is stepped-up, the value of voltage error is stepped-down. When *R* values more than 3 kΩ, the ECVT conforms to the standard transformer requirement. However, when the resistor divider increases continuously to 12 kΩ, its acts on voltage error will gradually flatten out. Besides, the further growth will restrain the elimination of the straight flow in secondary side voltage after reclosing.

During the reclosing simulation, the time interval and the phase of closing are the main factors leading to errors. Thus, the impact of the former on the transient error needs to be analyzed. The reclosing time interval is set at 0.2 s, 0.3 s, 0.4 s and 0.5 s respectively. The above process is repeated to simulate the relationship between the resistance R and the transient error at different time intervals, as shown in Figure 11.

As can be known from Figure 8, in the case of the same resistance, the longer the reclosing time interval, the larger the transient error. When the time interval is 0.5 s, the secondary load resistance must achieve to 5 kΩ to meet the standard requirements.

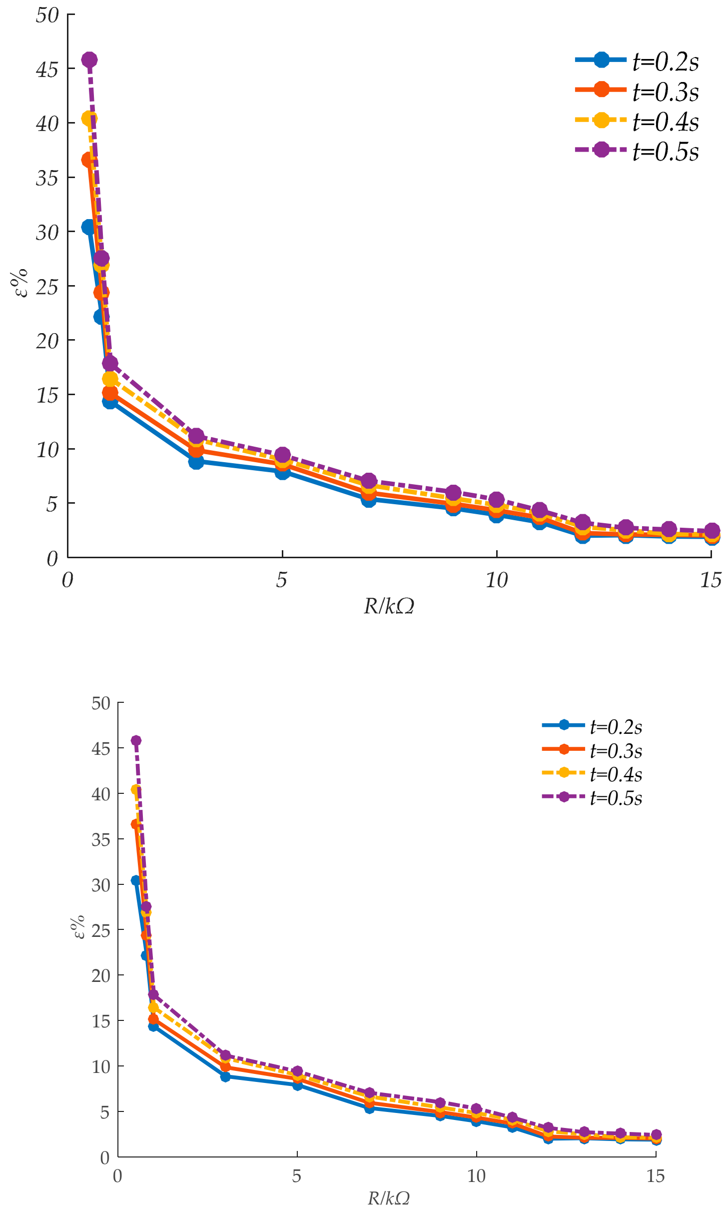

Figure 11. Relationship between resistor divider and the voltage error for different time interval.

4.2. Simulation Analysis of Transfer Characteristics

Through the theoretical analysis above, the frequency characteristic of ECVT is associated with its main component parameters. To fulfill the needs of ECVT transient characteristics, the range of the resistor divider is between 3 and 12 kΩ, and the corresponding frequency measurement range varies as shown in Figure 12.

From the analysis of Figures 5 and 6, we can see that its measurement range decreases with the increase of the value of the resistor divider. Furthermore, when R is equal to 5 kΩ, the normal measurement frequency range of the ECVT is about 10 to 10^4 rad/s (1.59~1.6 kHz), meet the19th harmonics measurement requirement specified in the utility grid harmonic power quality standards.

In the process of harmonic signal simulation test, the input voltage amplitude is the maximum value of the fundamental frequency voltage, and the initial phase is zero. The frequency is 1–19 times of the power frequency 50 Hz successively. Only alter the value of resistor divider R and the corresponding harmonic signal measurement errors of the ECVT at every single harmonic frequency are recorded. The result is exhibited in Figure 13.

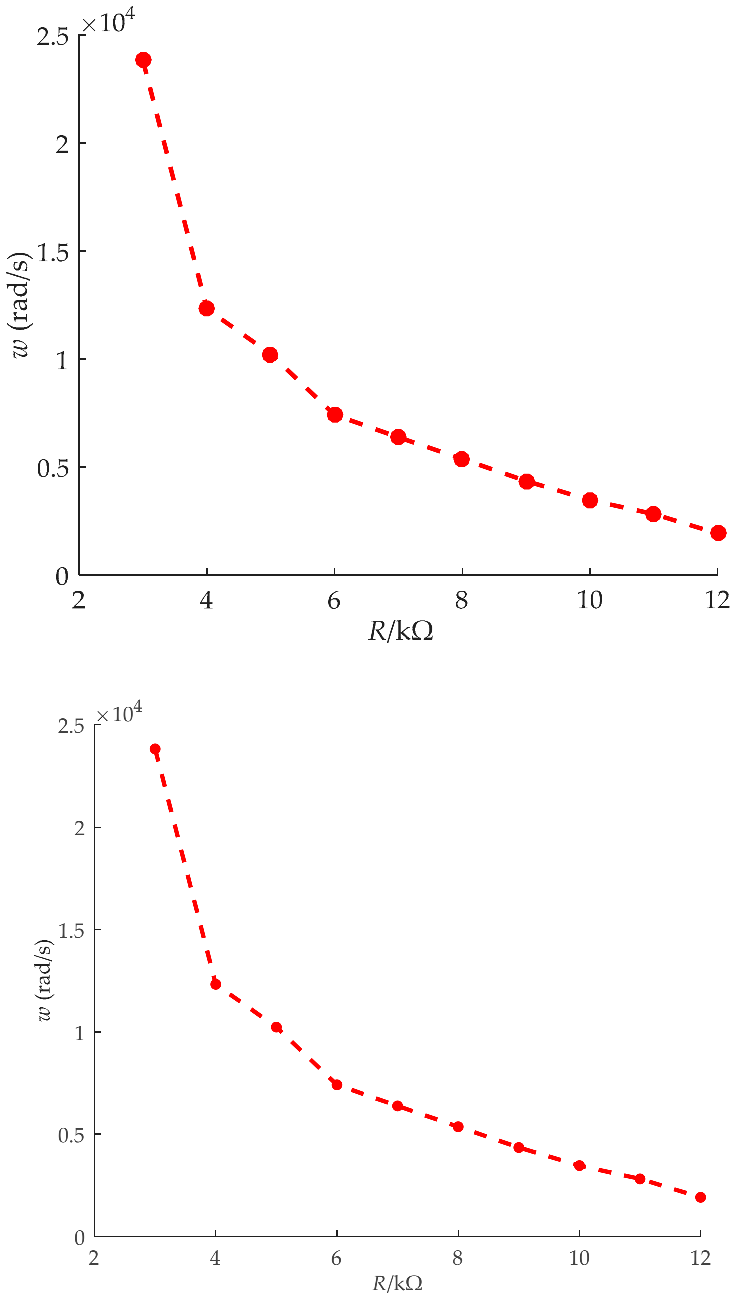

Figure 12. Relationship between resistor divider and frequency measurement range.

It can be perceived from Figure 13 that under the circumstances of primary voltage, the frequency is in the range of 50Hz to 950Hz, the alteration of the amplitude error fluctuation of secondary side voltage is consistent with the changing trend of the resistor divider. Furthermore, there is a sudden rise between the output amplitude error of the 17th and 19th harmonic at 6 kΩ. The same situation exists between the 15th and 17th harmonic at 7 kΩ. When the frequency of the harmonic signal exceeds the measurement bandwidth of ECVT, a large measurement error will occur in the secondary output signal. In this case, ECVT is unable to accurately measure the primary signal.

When the resistor divider R is 5 kΩ, its corresponding amplitude measurement errors are shown in Table 2. The output amplitude error of the ECVT does not exceed 0.42% under the condition of single harmonic voltage within the power frequency up to 950 Hz. The measured results satisfy the necessity of accurately 0.5 degrees for the ECVT.

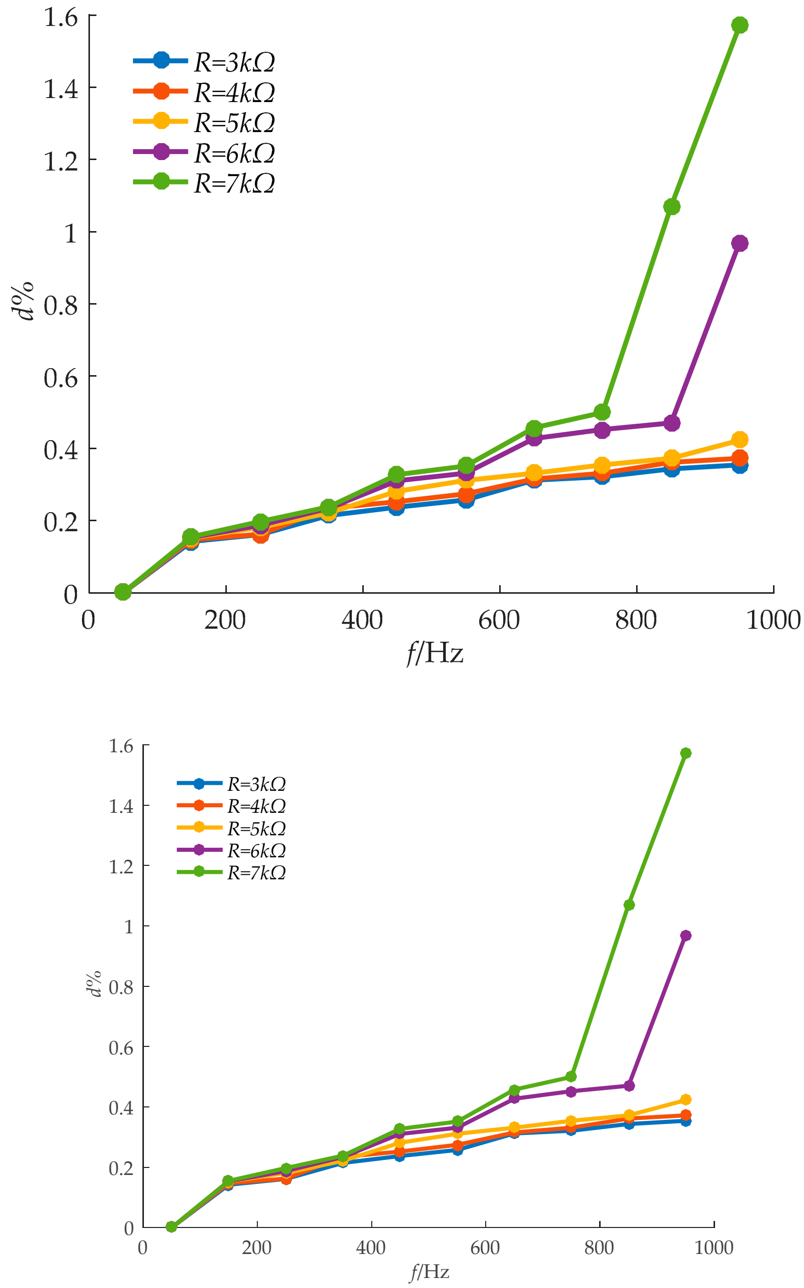

Figure 13. Relationship between harmonic and the voltage error for different divider resistance.

Table 2. Relationship between harmonic and voltage error.

Order of Harmonics	U_1/[kV]	U_o/[kV]	d/[%]
3	8.7406	0.005668	0.15
5	8.9332	0.005794	0.18
7	9.3123	0.006043	0.22
9	9.6416	0.00626	0.28
11	9.7925	0.00636	0.31
13	10.3152	0.006701	0.33
15	10.4322	0.006779	0.37
19	10.8766	0.007072	0.42

5. Parameter Optimization Design of ECVT

Minimization of decay duration and transient surge voltage and maximization of frequency bandwidth can be used as optimization targets for ECVT sensor design from the above analysis.

5.1. Target Function

5.1.1. Minimize Duration of Transient Voltage Attenuation

The charge is neutralized momentarily, and the remaining charge is discharged through resistor divider during short circuit and reclosing (Figure 7). Therefore, it is necessary to consider the effect of attenuation time constant on the power quality performance during the transient process.

$$\tau = RC_3 \tag{21}$$

5.1.2. Maximum Frequency Bandwidth

The frequency characteristics of the ECVT detectably affected the accuracy of its harmonic measurements. In this case, its performance improvement is associated with the upper limit cutoff frequency.

$$f_H = \frac{C_1 + 2C_2}{2\pi R C_n} \tag{22}$$

5.1.3. Minimize Transient Impulse Voltage

The impulse voltage not only exerts negative effects on transient performance, but also poses a threat to the safety and stability of ECVT at the moment of reclosing (Figure 8).

$$\Delta u_o(t) = \frac{1}{R_1 C} \cdot \frac{C_1 C_2}{C_n} \cdot RC_3 \cdot U_m \sin(2\pi f_n t_0) \cdot -e^{t_1/RC_3} \tag{23}$$

Considering the above three design objectives, the objective function is established as follows:

$$\min f_{(x)} = w_1 \tau - w_2 f_H + w_3 \Delta u_o(t) \tag{24}$$

Among them, ωwj is the weighting coefficient that reflects the importance of each sub-target. The entropy weight method is applied to obtain the value of each weighting coefficient [39,40]. The procedure is as follows:

(1) Basic process of each index data

Decay duration, transient surge voltage and frequency bandwidth are the three optimization indexes in this paper. Assuming that m samples are evaluated, the initial data matrix is

$$X = \begin{bmatrix} x_{11} & x_{12} & x_{13} \\ \vdots & \vdots & \vdots \\ x_{m1} & x_{m2} & x_{m3} \end{bmatrix},$$

$$X = \left\{x_{ij}\right\}_{m\times 3} \quad 0 \le i \le m, 0 \le j \le 3 \tag{25}$$

where x_{ij} is the value of the index j of the sample i.

(2) Data standardization

To eliminate the impact of different index dimensions and data levels on the evaluation results, each index is standardized. The normalized specific gravity matrix Y is proposed as

$$Y = \left\{y_{ij}\right\}_{m\times 3} \quad 0 \le i \le m, 0 \le j \le 3 \tag{26}$$

where $y_{ij} = (x_{ij} - \overline{x}_j / S_j) / \sum\limits_{i=1}^{m} (x_{ij} - \overline{x}_j / S_j)$, $0 \leq y_{ij} \leq 1$; $\overline{x}_j$ is the average value of index j; S_j is the standard deviation of index j.

(3) Calculate the information entropy value e and information utility value d

The information entropy value of index j can be calculated by Equation (27).

$$e_j = -K\sum_{i=1}^{m} y_{ij}\ln y_{ij} \tag{27}$$

where $K = 1/\ln m$.

The information utility value of index j can be calculated by Equation (28). The larger information utility values, the greater it affects to the evaluation and the greater its weight.

$$d_j = 1 + K\sum_{i=1}^{m} y_{ij}\ln y_{ij} \tag{28}$$

(4) Calculate the weight of evaluation index

The weight of the j evaluation index can be obtained by Equation (29)

$$w_j = \frac{d_j}{\sum\limits_{i=1}^{m} d_j} \tag{29}$$

Based on Equation (30), the comprehensive index value U_i of each sample is denoted as

$$U_i = \sum_{j=1}^{n} y_{ij}(X) w_j \tag{30}$$

According to the above calculation method, the linearly weighted objective function can be expressed as:

$$\min f_{(x)} = 0.4210\tau - 0.4472 f_H + 0.1318\Delta u_o(t) \tag{31}$$

5.2. Constraint Condition

5.2.1. Transient Voltage Error

As the measurement standard of ECVT transient performance, ε shall decrease to a specific value within three cycles after transient disturbance. Thus, after substituting the output voltage into Equation (11), the corresponding expression can be denoted as

$$\varepsilon = \frac{\frac{C_1 C_2}{C_n} \cdot U_m \cdot \sin(2\pi f_n t_o) \cdot e^{-(t-t_1)/RC_3} \times 100\%}{\sqrt{2} U_m \cdot \frac{wRC_1C_2}{C_1 + 2C_2}} \leq 10\% \tag{32}$$

5.2.2. Harmonic Measurement Error

The detection error caused by ECVT is reflected in amplitude measurement for high-frequency harmonics. Referring to the harmonic standard of power quality utility network, the amplitude measurement error should be less than 0.5%.

$$d = \frac{U_o - \frac{RC_1C_2}{CR_3(C_1+2C_2)} U_1}{U_o} \times 100\% \leq 5\% \tag{33}$$

5.2.3. Reclosing Time Interval

When resistor divider in ECVT is constant, the magnitude of the transient error is proportional to the length of the reclosing time interval (Figure 11). According to practical operating experience, the reclosing action time interval is usually 0.15 s to 0.5 s.

$$0.15 \leq \Delta t = t_1 - t_0 \leq 0.5 \tag{34}$$

5.3. Solution

Due to the repetitiveness and randomness of the traditional method of selecting parameters, the parameter solving process becomes complicated and difficult to implement. Therefore, the parameter design of ECVT sensor in this paper adopts genetic algorithm with high accuracy and takes the resistor divider R as the optimization variable to optimize. The specific optimization process is described in the literature [41]. Due to the limitation of length, there will be no more tautology here.

5.4. Optimization Results and Analysis

According to the data provided by Section 4 and other hardware parameters of the ECVT, its power quality detection capability is optimized by genetic algorithm. The maximum number of iterations is 150, and the population size is 50. The optimization result of ECVT sensor parameters is 4.237 kΩ. Based on the simulation model of Section 4, the optimization result of resistor divider is substituted into it. Besides, the rated input voltage is $10/\sqrt{3}$ kV; fundamental frequency f_n is 50 Hz; short circuit occurs at peak voltage; the reclosing time interval is 0.15 s. In short circuit simulation, the transient characteristic of ECVT is shown in Figure 14a. In the reclosing simulation, the action time and time interval are consistent with Section 4. The reclosing waveform is demonstrated in Figure 14b. Moreover, the transient voltage errors in the two simulations are both less than 10%, which meets the requirements of the transformer standard. Output amplitude errors of ECVT within the power frequency up to 950 Hz are presented in Table 3. The maximum error does not exceed 0.5%. Analysis of those performances showed that the ECVT has high accuracy in restoring the primary signal.

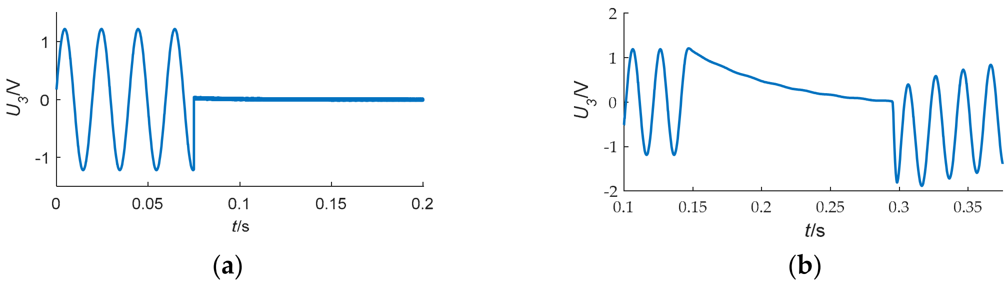

Figure 14. (**a**) Short circuit waveform of ECVT and (**b**) Reclosing waveform of ECVT.

Table 3. Relationship between harmonic and voltage error.

Order of Harmonics	U_1/[kV]	U_o/[kV]	d/[%]
3	8.9401	0.00583	0.13
5	8.9062	0.005807	0.15
7	9.5228	0.006205	0.21
9	9.7441	0.006345	0.28
11	9.8915	0.00644	0.30
13	10.2182	0.00665	0.33
15	10.3312	0.006721	0.38
19	10.7716	0.007006	0.40

6. Discussion

The transient performance and transmission characteristics of ECVT are theoretically deduced. It is found that the value of resistor divider will directly affect the decay time constant of the trapped charge and the error between secondary voltage after reclosing and its steady state voltage. On the one hand, when the circuit breaker is disconnected, the low voltage side capacitor will discharge through the resistor divider. The voltage difference generated in this process will cause the transient disturbance voltage after closing. On the other hand, at the beginning of closing, the DC voltage component superimposed on the secondary voltage will discharge through the resistance R. The discharge time will directly determine the magnitude of voltage error. Meanwhile, the upper limit of the normal frequency measurement range of ECVT is highly correlated with the value of resistor divider. Therefore, the transient voltage error and the frequency bandwidth of ECVT are inextricably linked with the resistor divider, the addition of which modifies the transient performance and transmission characteristics of ECVT. The resistor divider becomes the key parameter affecting the performance of ECVT power quality detection.

Through further simulation analysis, it can be perceived that in the occasions of two prominent transient problems, short circuit and reclosing, the decline of resistor divider R could reduce the decay time constant and shorten transient process. In addition, short circuit occurrence time and reclosing time interval are also significant factors to the ECVT transient characteristics. Meanwhile, the upper limit of its normal frequency measurement range enhances with the reduction of R. When the harmonic frequency exceeds the measured frequency range, the secondary output voltage will produce a large error. As the value of the resistor divider decreases, its influence on the overall partial voltage ratio and phase error of ECVT will gradually increase. If the resistance is too small, the transient may even result in overvoltage and damage to the circuit device. Results show that the outcomes of the decay time constant, frequency measurement range and overvoltage are the three principal factors that determine the value range of parameter R. On this basis, a multi-objective optimization model is established, and genetic algorithm is used to solve the model. For 10 kV ECVT that is purposed in this article, its accuracy class is 0.5 degrees. As can be noticed from Figure 10, there is an optimum value of the resistor divider of capacitive voltage divider in the range of 3–5 kΩ. Through the proposed parameter optimization method, the optimal value obtained is 4.237 kΩ. Furthermore, the transient error fulfills the requirements of ECVT (Table 3). The ECVT not only has the functions of conventional voltage measurement and relay protection, but also can truthfully reflect the harmonic and transient disturbance signals up to 19 times, meeting the requirements of broadband and high precision detection of power quality for distribution network.

At present, there is still a broader space for development for research on the optimum design of ECVT. Further research is needed in respects of series resistance of voltage divider capacitance, changes in environmental conditions such as rain, snow, temperature and humidity as well as the degree of asymmetry in the way the system operates. Accurate electrical measurement technology is still the premise for the reliable and safe development of power system and the key link to ensure its economic operation.

7. Conclusions

Transient performance and harmonic signal transfer capability are the important factors of ECVT performance. In this paper, the impacts of those two factors are studied, according to the International Electro technical Commission standard definition of electronic voltage transformer transient error, by using the established mathematical model of ECVT sensor. Then, the influence rule and the change characteristics of the resistor divider on transient voltage error and normal frequency measurement range are analyzed. Those findings could provide reference data for the performance analysis and make its design more reasonable. The ECVT of the 10 kV system is simulated with Simulink platform. It was found that the outcomes of the decay time constant, frequency measurement range and overvoltage are the three principal factors that form constraints on the value range of parameter R. On this basis, a multi-objective optimization parameter optimization design model is carried out. The optimal parameter value obtained by entropy weight method and genetic algorithm is 4.237 kΩ. The numerical result of transient voltage error is in the allowable range of transformer standard and the ECVT realizes a measurement of the power frequency and 2–19 times single harmonic voltage signals.

Author Contributions: Methodology, Y.Z. and X.Z.; Validation, Y.Z., and B.A.; Formal Analysis, Y.Z.; Investigation, Y.Z.; Data Curation, Y.Z.; Software, X.Z.; Writing—Original Draft Preparation, Y.Z. and X.Z.; Writing—Review and Editing, Y.Z.; Visualization, X.L.; Supervision, X.L. and B.A.; Project Administration, X.L.

Funding: This research received no external funding.

Conflicts of Interest: The authors declare no conflict of interest.

References

1. Luo, A.; Xu, Q.M.; Ma, F.J.; Chen, Y.D. Overview of power quality analysis and control technology for the smart grid. *J. Mod. Power Syst. Clean Energy* **2016**, *4*, 1–9. [CrossRef]
2. Otcenasova, A.; Bolf, A.; Altus, J.; Regula, M. The Influence of Power Quality Indices on Active Power Losses in a Local Distribution Grid. *Energies* **2019**, *12*, 1389. [CrossRef]
3. Ghassemi, F.; Gale, P.; Cumming, T.; Coutts, C. Harmonic voltage measurements using CVTs. *IEEE Trans. Power Deliv.* **2005**, *20*, 443–449.
4. Le, J.; Liu, Y.Z.; Li, Q.L. Harmonic measurement error test technology of capacitive voltage transformer. *Autom. Electr. Power Syst.* **2016**, *40*, 108–113.
5. Duan, X.Y.; Liao, M.F.; Zou, J.Y. Electronic voltage transformers based on capacitive voltage divider. *High Volt. Eng.* **2003**, *29*, 50–59.
6. Chen, R.Y.; Wang, Z.X. Abnormal Growth Analysis of Dielectric Loss Factor in Capacitor Voltage Transformer. *Power Syst. Clean Energy* **2012**, *28*, 4.
7. Schmid, J.; Kunde, K. Application of non-conventional voltage and currents sensors in high voltage transmission and distribution systems. In Proceedings of the 2011 IEEE International Conference on Smart Measurements of Future Grids (SMFG) Proceedings, Bologna, Italy, 14–16 November 2011; pp. 64–68.
8. Nie, Y.X.; Sun, D.T. Characteristic Analysis of Resistive-Capacitive Divider Voltage Transformer. *Transformer* **2007**, *1*, 2.
9. Bertolotto, P.; Faifer, M.; Ottoboni, R. High voltage multi-purpose current and voltage electronic transformer. In Proceedings of the 2007 IEEE Instrumentation & Measurement Technology Conference (IMTC), Warsaw, Poland, 1–3 May 2007; pp. 1–5.
10. Liang, Y.; Huang, X.; Chen, C. The cause of TV secondary wire abnormity and its countermeasures. *Electr. Power Autom. Equip.* **2001**, *21*, 73–74.
11. Wang, J.; Guo, Z.; Zhang, G.; Wang, G.; Yu, W.; Shen, Y. Investigation and simulation of transient characteristics of electronic voltage transformer. *Electr. Power Autom. Equip.* **2012**, *32*, 62–65.
12. Liu, Q.; Xu, Y.; Gao, F. Simulation research on electronic voltage transformer transient process. *J. Electr. Eng.* **2015**, *10*, 39–43.
13. Xu, Z.C.; Yang, L.J.; Li, X.M. Simulation Study on Measurement Performance of Disturbance Signal of Electronic Capacitive Voltage Transformer. *High Volt. Appar.* **2015**, *51*, 91–96.
14. Cataliotti, A.; Cosentino, V.; Crotti, G.; Giordano, D.; Modarres, M.; Di Cara, D.; Luiso, M. Metrological performances of voltage and current instrument transformers in harmonics measurements. In Proceedings of the 2018 IEEE International Instrumentation and Measurement Technology Conference (I2MTC), Houston, TX, USA, 14–17 May 2018; pp. 1–6.
15. Yao, X.; Bin, H.; Chunnian, D. Problems of voltage transducer in harmonic measurement. In Proceedings of the 10th International Conference on Harmonics and Quality of Power Proceedings (Cat. No. 02EX630), Rio de Janeiro, Brazil, 6–9 October 2002; Volume 1, pp. 33–37.
16. Pawelek, R.; Wasiak, I. Comparative measurements of voltage harmonics in transmission grid of 400 kV. In Proceedings of the 2014 16th International Conference on Harmonics and Quality of Power (ICHQP), Bucharest, Romania, 25–28 May 2014; pp. 606–610.
17. Yang, L.; Zhou, D.; Xu, Z. Characteristics of electronic voltage transformers based on capacitive voltage divider. *Electr. Power Autom. Equip.* **2012**, *32*, 71–74.

18. Brandolini, A.; Faifer, M.; Ottoboni, R. A simple method for the calibration of traditional and electronic measurement current and voltage transformers. *IEEE Trans. Instrum. Meas.* **2009**, *58*, 1345–1353. [CrossRef]
19. Bakar, A.H.A.; Lim, C.H.; Mekhilef, S. Investigation of transient performance of capacitor voltage transformer. In Proceedings of the 2006 IEEE International Power and Energy Conference, Putra Jaya, Malaysia, 28–29 November 2006; pp. 509–515.
20. Metwally, I.A. Failures, monitoring and new trends of power transformers. *IEEE Potentials* **2011**, *30*, 36–43. [CrossRef]
21. Koch, M.; Prevost, T. Analysis of dielectric response measurements for condition assessment of oil-paper transformer insulation. *IEEE Trans. Dielectr. Electr. Electr.* **2012**, *19*, 1908–1915. [CrossRef]
22. Liu, X.; Guo, K.Q.; Ye, G.X.; Huang, H.; Yang, F.; Chen, P. Experimental study on the impulse-voltage transmission characteristics of inductive voltage transformers. *Gaodianya Jishu/High Volt. Eng.* **2011**, *37*, 2385–2390.
23. Wang, H.X.; Zhang, G.Q.; Cai, X.G. Study on error Characteristics of EVT in power system and Optimum design of EVT parameter. *Guangdong Electr. Power* **2011**, *12*, 85–91.
24. Stiegler, R.; Meyer, J.; Kilter, J.; Konzelmann, S. Assessment of voltage instrument transformers accuracy for harmonic measurements in transmission systems. In Proceedings of the 2016 17th International Conference on Harmonics and Quality of Power (ICHQP), Belo Horizonte, Brazil, 16–19 October 2016; pp. 152–157.
25. Feng, Y.U.; Wang, X.Q.; Chen, X.M. Influence of circuit parameters of capacitor voltage transformer on grid harmonic voltage measurements. *Proc. CSEE* **2014**, *34*, 4968–4975.
26. Xiong, X.F.; He, N.; Yu, J.; HU, Z.R. Diagnosis of abrupt-changing fault of electronic instrument transformer in digital substation based on wavelet transform. *Power Syst. Technol.* **2010**, *34*, 181–185.
27. Yazdani, A.; Iravani, R. *Voltage-Sourced Converters in Power Systems*; John Wiley & Sons: Hoboken, NJ, USA, 2010; Volume 34.
28. Qing, C.; Li, H.-B.; Huang, B.-X. An innovative combined electronic instrument transformer applied in high voltage lines. *Measurement* **2010**, *43*, 960–965. [CrossRef]
29. Zhang, M.M.; Zhang, C.S.; Li, C. The Simulation and Research Based on the Digital Integrator of the ECVT. *Electron. Sci. Technol.* **2018**, *31*, 17–19.
30. Wang, H.B.; Zhao, Z.M. Research of electronic voltage transformer based on capacitive voltage divider. *Relay* **2007**, *35*, 46–49.
31. Faifer, M.; Ottoboni, R. An electronic current transformer based on Rogowski coil. In Proceedings of the 2008 IEEE Instrumentation and Measurement Technology Conference, Victoria, BC, Canada, 12–15 May 2008; pp. 1554–1559.
32. Li, W.; Yin, X.; Chen, D.; Zhang, Z.; Chen, W. The study of transient performance for electronic current transformer sensor based on Rogowski coil. In Proceedings of the 41st International Universities Power Engineering Conference, Newcastle, UK, 6–8 September 2006; Volume 1, pp. 162–165.
33. Abyaneh, H.A.; Kamangar, S.S.H.; Razavi, F.; Chabanloo, R.M. A new genetic algorithm method for optimal coordination of overcurrent relays in a mixed protection scheme with distance relays. In Proceedings of the 2008 43rd International Universities Power Engineering Conference, Padova, Italy, 1–4 September 2008; pp. 1–5.
34. Tan, B.H.; Allen, N.L.; Rodrigo, H. Progression of positive corona on cylindrical insulating surfaces. I. Influence of dielectric material. *IEEE Trans. Dielectr. Electr. Insul.* **2007**, *14*, 111–118. [CrossRef]
35. Luo, S.; Ye, M. Research Development of Electronic Transducer. *Jiangsu Electr. Eng.* **2003**, *22*, 51–54.
36. Li, T.; Du, X.P.; Liu, H.G. Discussion about self-excited method error on capacitive voltage transformer. *Power Syst. Prot. Control.* **2009**, *37*, 31–33.
37. Ahn, S.P.; Kim, C.H.; Aggarwal, R.K.; Johns, A.T. An alternative approach to adaptive single pole auto-reclosing in high voltage transmission systems based on variable dead time control. *IEEE Trans. Power Syst.* **2001**, *16*, 676–686. [CrossRef]
38. Ali, M.H.; Murata, T.; Tamura, J. Transient stability enhancement by fuzzy logic-controlled SMES considering coordination with optimal reclosing of circuit breakers. *IEEE Trans. Power Syst.* **2008**, *23*, 631–640. [CrossRef]
39. Kamiński, M. Tsallis entropy in dual homogenization of random composites using the stochastic finite element method. *Int. J. Numer. Methods Eng.* **2018**, *113*, 834–857. [CrossRef]

40. Shi, T.Y.; Wang, D.Z.; Li, Z. Multi-objective optimization design of PMECD by multiple population genetic algorithm. *Trans. China Electron. Technol. Soc.* **2016**, *31*, 262–268.
41. Xiao, X.; Xu, Q.S.; Wang, Y.T. Parameter identification of interior permanent magnet synchronous motors based on genetic algorithm. *Trans. China Electron. Technol. Soc.* **2014**, *29*, 21–26.